

Fission fragment isomers populated via  ${}^6\text{Li} + {}^{232}\text{Th}$ 

J. J. Ressler,<sup>1</sup> J. A. Caggiano,<sup>1</sup> C. J. Francy,<sup>1,2</sup> P. N. Peplowski,<sup>1</sup> J. M. Allmond,<sup>3</sup> C. W. Beausang,<sup>3</sup> L. A. Bernstein,<sup>4</sup> D. L. Bleuel,<sup>4</sup> J. T. Harke,<sup>4</sup> P. Fallon,<sup>5</sup> A. A. Hecht,<sup>6</sup> D. V. Jordan,<sup>1</sup> S. R. Leshner,<sup>4,\*</sup> M. A. McMahan,<sup>5,†</sup> T. S. Palmer,<sup>2</sup> L. Phair,<sup>5</sup> N. D. Scielzo,<sup>4</sup> P. G. Swearingen,<sup>1,2</sup> G. A. Warren,<sup>1</sup> and M. Wiedeking<sup>4</sup>

<sup>1</sup>*Pacific Northwest National Laboratory, Richland, Washington 99352, USA*

<sup>2</sup>*Department of Nuclear Engineering, Oregon State University, Corvallis, Oregon 97331, USA*

<sup>3</sup>*Department of Physics, University of Richmond, Richmond, Virginia 23173, USA*

<sup>4</sup>*Lawrence Livermore National Laboratory, Livermore, California 94551, USA*

<sup>5</sup>*Lawrence Berkeley National Laboratory, Berkeley, California 94720, USA*

<sup>6</sup>*Department of Nuclear Engineering, University of New Mexico, Albuquerque, New Mexico 87131, USA*

(Received 28 September 2009; published 6 January 2010)

Short-lived isomers in fission fragments following bombardment of 45-MeV  ${}^6\text{Li}$  on  ${}^{232}\text{Th}$  were examined. Isomers in the  $A \sim 95$ , 122, and 132 mass regions were observed. New isomeric decays were observed in  ${}^{121}\text{In}$  [ $T_{1/2} = 17(2) \mu\text{s}$ ],  ${}^{123}\text{In}$  ( $T_{1/2} \gtrsim 100 \mu\text{s}$ ), and  ${}^{125}\text{Sb}$  [ $T_{1/2} = 25(4) \mu\text{s}$ ]. These isomers are suggested to arise from  $\nu(h_{11/2} \otimes d_{3/2})7^-$  and  $\nu(h_{11/2} \otimes s_{1/2})5^-$  neutron core excitations coupling with the valence proton.

DOI: [10.1103/PhysRevC.81.014301](https://doi.org/10.1103/PhysRevC.81.014301)

PACS number(s): 24.75.+i, 21.10.Tg

## I. INTRODUCTION

Nuclear structure studies of neutron-rich nuclei provide much-needed data to test the predictive power of theoretical models. These nuclei are difficult, if not impossible, to produce in standard fusion-evaporation reactions. Nuclei close to stability may be investigated with deep inelastic reactions, while more neutron rich isotopes may be studied following  $\beta$  decay following fragmentation or fission.

Fission has been used extensively to study neutron-rich nuclei, particularly in the production of the  $\beta$ -decay parents. Spontaneous fission, thermal neutrons on fissile isotopes, and relativistic fission of actinides on light targets have produced a plethora of information on many neutron-rich isotopes.

In this paper, intermediate-energy fission using an energetic light ion ( ${}^6\text{Li}$ ) on an actinide target ( ${}^{232}\text{Th}$ ) was used to populate neutron-rich isotopes. Fission is expected to dominate the reaction profile, with an estimated cross section of  $\sim 600$  mb [1]. A number of isotopes through symmetric and antisymmetric fission were produced, notably in the  $A = 100$ , 122, and 132 mass regions.

Numerous isomers in the neutron-rich nuclei were populated in the fission reaction. The presence of nuclear isomers is an interesting structural phenomenon, arising from small decay energies, large changes in angular momentum, and/or significant structural differences.

Of particular interest, the fission reaction allowed a broad study of microsecond isomers in the  $Z \sim 50$  isotopes with  $A \sim 122$ . Isomers attributed to  $\nu(h_{11/2} \otimes d_{3/2})7^-$  and  $\nu(h_{11/2} \otimes s_{1/2})5^-$  excitations are expected to dominate the isomer landscape in this mass region. Decays from these states are

well understood in the Sn isotopes, but data in the neighboring  $Z = 51$  (Sb) and  $Z = 49$  (In) are more sparse. New isomers in  ${}^{121}\text{In}$ ,  ${}^{123}\text{In}$ , and  ${}^{125}\text{Sb}$ , proposed in this paper, help to complete the systematic behavior of these neutron excitations.

## II. EXPERIMENT

An isotopically pure,  $889 \mu\text{g}/\text{cm}^2$   ${}^{232}\text{Th}$  target was bombarded with a 45-MeV beam of  ${}^6\text{Li}$  ions from the 88-Inch Cyclotron at Lawrence Berkeley National Laboratory. Following the reaction, emitted particles and fission fragments were detected in the Silicon Telescope Array for Reaction Studies (STARS) [2,3]. The STARS array comprises a series of double-sided annular Si detectors for particle detection. For this study, the array consisted of three detectors downstream of the target for reaction channel identification and a fourth detector, upstream from the target, for fission tagging.

The downstream detectors, denoted as  $\Delta E$ ,  $E1$ , and  $E2$ , consisted of  $140\text{-}\mu\text{m}$ ,  $994\text{-}\mu\text{m}$ , and  $1001\text{-}\mu\text{m}$ -thick detectors, respectively. This telescope array covered a range from  $21^\circ$  to  $52^\circ$  at forward angles, relative to the beam axis. A  $130\text{-}\mu\text{m}$ -thick stainless-steel shield was placed in front of the telescope array to slow the hydrogen species (protons, deuterons, and tritons) and stop scattered  ${}^6\text{Li}$  beam ions. This shield was also used to protect the  $\Delta E$  Si detector from  $\delta$  electrons emitted from the target. Similar shields, composed of  $4 \text{ mg}/\text{cm}^2$  Al, were placed behind the  $E1$  detector and in front of the  $E2$  detector. A thick Al shield ( $\sim 1.6$  mm) was placed behind the  $E2$  detector. All shields were biased to  $+300$  V. The particle array detected hydrogen and helium isotopes emitted in the reaction.

Coincident  $\gamma$  rays were detected in the Livermore Berkeley Array for Collaborative Experiments [4,5]. This array consisted of six clover HPGe detectors and one low-energy photon spectrometer (LEPS). Five clovers and the single LEPS were placed around the target chamber in a single plane parallel to the beam axis. The sixth clover was mounted above the

\*Current address: Department of Physics, University of Wisconsin, LaCrosse, Wisconsin 54601, USA.

†Current address: South Dakota Science and Technology Authority, Sanford Underground Science and Engineering Laboratory at Homestake, Lead, South Dakota 57754, USA.

target chamber, perpendicular to the remainder of the array. Because of the thick target chamber,  $\gamma$  rays below  $\sim 150$  keV were highly attenuated.

To identify isomeric decays, the beam was intermittently blocked, or “chopped.” A square-pulse generator was used to create the desired waveform for the beam on/off periods. This signal was used to drive an electrostatic switch located between the ion source and the injection point of the cyclotron. For this study, the beam was on target for 32  $\mu$ s, then blocked for 148  $\mu$ s.

Isomeric states were populated while the beam was on target, and the decay was observed while the beam was blocked. Particles detected during the beam-on period were correlated to  $\gamma$  events during the beam-off period. With the beam structure as described, correlation times from 0 to 180  $\mu$ s are possible.

The correlation time between events was registered using a time-to-amplitude converter (TAC) or a 50-MHz Fast Encoding and Readout ADC (FERA) clock in the data stream. The data acquisition system was started by a particle event in the Si telescope, or a  $\gamma$  event coincident with the beam-off signal. Each event type had a time stamp from the FERA clock, and correlation times were simply the time difference between the particle and  $\gamma$  events.

Following a particle event, the data acquisition system was busy processing data and could not detect subsequent  $\gamma$  events quickly. To alleviate this issue, the TAC was used. A particle detected in the Si telescope started the TAC; the TAC was then stopped by a  $\gamma$  coincident with the beam-off signal. If a  $\gamma$  ray was not detected within 45  $\mu$ s after a particle event, the TAC self-cleared. The event was constructed such that the particle read-out did not occur until after the TAC cleared. This delayed the particle dead time to the end of the event, allowing short-lived isomeric decays to be observed.

Collected data were sorted into  $\gamma$ - $\gamma$ ,  $\gamma$ -time, and time-gated  $\gamma$ - $\gamma$  matrices for analysis. The current study was sensitive to microsecond isomers in fission fragments from  $A \sim 90$  through  $A \sim 150$ . The largest isomer populations are attributed to  $Z \sim 39$  (Y) with  $A \sim 95$ ,  $Z \sim 50$  (Sn) with  $A \sim 122$ , and  $Z \sim 54$  (Xe) with  $A \sim 132$ .

Particle- $\gamma$  correlations from 5 to 175  $\mu$ s were successfully examined. Correlations at the extremes of the coincidence window were hampered by the low detection probability. For example, for early particle- $\gamma$  correlations the particle would need to be detected near the end of the beam-on period, and the  $\gamma$  near the start of the beam-off period.

### III. RESULTS

Numerous isomers were observed in this study, and a summary of identified decays is provided in Table I. A significant contribution from symmetric fission, populating isomers near  $A \sim 122$ , is observed. Symmetric fission is not unexpected at the high bombardment energy; mass peaks at  $A = 100, 120,$  and  $138$  were observed in a similar reaction using 40-MeV  ${}^6\text{Li}$  ions on  ${}^{232}\text{Th}$  [6].

Time subtractions were performed to isolate short-lived isomeric transitions by removing longer lived species, such as those following  $\beta$  decay or arising from room background.

Examples of such subtractions are shown in Fig. 1. Isomers with half-lives in the general range of  $5 \lesssim T_{1/2} \lesssim 100$   $\mu$ s can be observed. Sensitivity to shorter half-lives ( $< 5$   $\mu$ s) requires significant production in the fission reaction for observation.

New isomeric transitions were observed in  ${}^{121}\text{In}$  and  ${}^{125}\text{Sb}$  and are proposed for  ${}^{123}\text{In}$ . While decay schemes can be built with relative ease, measurements of isomer half-lives were challenging due to the density of peaks and significant background. Decay data were corrected for the detection probability prior to exponential fitting.

#### A. ${}^{121}\text{In}$

Four  $\gamma$  rays, with energies of 1182, 953, 214, and 99 keV, were assigned to an isomeric decay in  ${}^{121}\text{In}$ . All four transitions are mutually coincident, suggesting a direct decay path to ground or another long-lived level. An example of coincidences with the 1182-keV transition is shown in Fig. 2.

The 1182-keV transition is known previously from the  ${}^{121}\text{Cd}$   $\beta$  decay [41] and light-ion reactions on  ${}^{124}\text{Sn}$  [42] and is suggested as the decay from a  $J^\pi = 13/2^+$  state at 1182-keV excitation energy to the  $9/2^+$  ground state. The  $\beta$ -decay experiment also observed the 953-keV  $\gamma$  ray in coincidence with the 1182-keV transition.

From a comparison to neighboring In isotopes, the isomeric state is suggested to have  $J^\pi = 21/2^-$  spin and parity at an excitation energy of 2448 keV. This decay feeds a  $17/2^-$  level at 2234 keV. The  $17/2^-$  state is not observed to be isomeric, with a 99-keV de-excitation. Assuming a single decay chain, intensities of the 214-, 99-, 953-, and 1182-keV  $\gamma$  rays should be equal. Missing intensity in the 99-keV transition was attributed to electron conversion. The conversion of the 99-keV  $\gamma$  ray suggests an  $M1$  or  $E2$  character ( $\alpha \sim 1.14$ ). The proposed decay scheme is shown in Fig. 3. Note that the order of the 99- and 214-keV isomeric decay  $\gamma$  rays observed in this paper is not known. It is suggested that the 214-keV transition directly depopulates the isomer, followed by the 99-keV transition, from a comparison to neighboring nuclei.

Negative-parity isomers are observed in most odd- $A$  nuclei near  $N = 82$ . In the In isotopes, known isomers have spins of  $17/2^-$ ,  $21/2^-$ , or  $23/2^-$ . Positive-parity isomers, with  $J^\pi = 25/2^+$  or  $29/2^+$  are also observed, at higher excitation energies relative to the negative-parity isomers. A direct decay path to the ground state was observed in this paper, suggesting that the measured isomer has negative parity.

These four transitions were also found to be isomeric in a recent high-spin study of  ${}^{121}\text{In}$  [43]. In that work the 99-keV transition was assigned as a decay from a  $J^\pi = 25/2^+$  isomer, followed by the 214-, 953-, 1182-keV, and a series of unobserved low-energy transitions.

The isomeric half-life observed by Ref. [43] was  $350 \pm 50$  ns. Such a short decay time is impossible to see in the current setup, and a different state is likely being populated. A half-life of  $17 \pm 2$   $\mu$ s was determined from fits to the decay of the 1182-, 953-, and 214-keV data in the current experiment.

It is possible that the 17- $\mu$ s isomer observed here is at a higher excitation energy than the  $J^\pi = 25/2^+$  isomer of Ref. [43]. The 17- $\mu$ s decay may proceed through an unobserved transition to the 350-ns isomer and follow the decay

TABLE I. Assigned isomeric  $\gamma$  decays observed in this experiment. For each isotope, the half-life ( $T_{1/2}$ ), initial excitation energy ( $E_i$ ), final excitation energy ( $E_f$ ), and delayed decay transitions ( $E_\gamma$ ) are shown. Transitions marked with an asterisk (\*) are assigned to the decay chain but are too low in energy to be observed in this study. For isomers with a single  $\gamma$ -ray emission, isotopic identification is uncertain. With the exception of  ${}^{121}\text{In}$ ,  ${}^{123}\text{In}$ , and  ${}^{125}\text{Sb}$ , half-lives shown are literature values.

Isotope	$T_{1/2}$ ( $\mu\text{s}$ )	$E_i$ (keV)	$E_f$ (keV)	$E_\gamma$ (keV)	Ref.
${}^{88}\text{Br}$	5.3(4)	270	0	111, 159	[7–9]
${}^{93}\text{Rb}$	57(15)	253	0	253	[7]
${}^{95}\text{Y}$	56.2(1.5)	1088	0	261, 827	[10–12]
${}^{98}\text{Y}$	0.62(8)	171	0	171	[9]
	7.6(4)	496	171	121	[7–9]
${}^{99}\text{Y}$	8.6(8)	2142	0	125, 214, 273, 1530	[13]
${}^{99}\text{Mo}$	15.5(2)	98	0	98	[14]
${}^{100}\text{Tc}$	8.32(14)	201	0	29*, 172	[15,16]
${}^{121}\text{In}$	17(2)	2348	0	99, 214, 953, 1182	This work
${}^{123}\text{In}$	1.4(2)	2079	0	32*, 881, 1020, 1027, 1166	[17]
	$\geq 100$	2079+x	2079	x	This work
${}^{119}\text{Sn}$	9.6(1.2)	2127	90	818, 1220	[18]
${}^{120}\text{Sn}$	11.8(5)	2482	0	90, 197, 1023, 1171	[19,20]
	6.26(11)	2902	2482	66*, 355	[20]
${}^{121}\text{Sn}$	5.3(5)	1999	0	841, 1151	[21]
${}^{122}\text{Sn}$	7.5(9)	2409	0	104, 163, 1001, 1140	[22,23]
	62(3)	2766	2409	75, 281	[24]
${}^{123}\text{Sn}$	7.4(2.6)	1945	0	728, 820, 838, 1107, 1217	[18]
	6	2153	1945	208	[21,25]
${}^{124}\text{Sn}$	0.27(6)	2205	0	103, 969, 1073, 1132	[22]
	3.1(5)	2325	2205	120	[22]
	45(5)	2657	2325	78, 253	[22]
${}^{125}\text{Sn}$	6.2(2)	1894	0	661, 792, 806, 1088, 1219	[26,27]
${}^{126}\text{Sn}$	6.6(1.1)	2219	0	57*, 112, 909, 1141	[22]
	7.7(5)	2565	2219	76, 269	[28]
${}^{127}\text{Sn}$	4.5(2)	1894	0	715, 1095	[26,27,29]
${}^{123}\text{Sb}$	64(1)	2613	0	128, 442, 956, 1089	[30,31]
${}^{125}\text{Sb}$	25(4)	1969+x	0	x, 880, 902, 1067, 1089	This work
${}^{127}\text{Sb}$	11(1)	1920	0	806, 825, 1095, 1114	[32]
${}^{131}\text{Sb}$	91(4)	1676	0	450, 1226	[10,33]
${}^{131}\text{I}$	24(1)	1918	0	122, 200, 241, 330, 773, 782, 823	[34]
${}^{132}\text{Te}$	0.145(8)	1775	0	104, 141, 697, 974	[35]
	28.1(1.5)	1925	1775	151	[36]
${}^{134}\text{Xe}$	5(1)	3026	0	28*, 405, 847, 861, 884	[37]
${}^{136}\text{Xe}$	2.95(9)	1891	0	197, 381, 1313	[7,12,38–40]

scheme suggested by Ref. [43]. The two isomers would rapidly reach secular equilibrium (within  $\sim 2 \mu\text{s}$ ), and only the 17- $\mu\text{s}$  decay half-life would be observed. However, such a high-spin, high-energy isomer would not be expected in  ${}^{121}\text{In}$ ; therefore, further work to clarify the decay scheme is necessary.

### B. ${}^{123}\text{In}$

Delayed transitions in  ${}^{123}\text{In}$  were also observed. There is a known isomer at 2079-keV excitation energy [17] that de-excites via a 32-keV  $\gamma$  ray to a level at 2047 keV. Two decay paths, each with a pair of  $\gamma$  rays, are reported. One path populates the  $11/2^+$  level at 1027 keV while the other populates the  $13/2^+$  state at 1166 keV. The decay sequence for the higher energy  $\gamma$  rays was confirmed in the current experiment.

A relatively short half-life, only 1.4  $\mu\text{s}$ , was reported for the isomeric state. Decays from an isomer with this half-life

would be difficult to observe in the present setup; therefore, it is likely that a longer lived state resides above the 1.4- $\mu\text{s}$  isomeric level, further delaying the decays observed here. The energy level scheme is shown in Fig. 3.

By assuming a single transition between the two isomeric states, it is not possible to assign this transition in the current experiment. Mass separation or isomer decay tagging would be needed to determine the origin with confidence.

The half-life of the proposed long-lived state could not be determined from the decay times of the known  $\gamma$  rays. The intensity in the time spectra suggests a significantly long half-life,  $\geq 100 \mu\text{s}$ .

### C. ${}^{125}\text{Sb}$

Four delayed transitions, suggested as decays in  ${}^{125}\text{Sb}$ , were observed.  $\gamma$  rays of 1089 and 880 keV were coincident

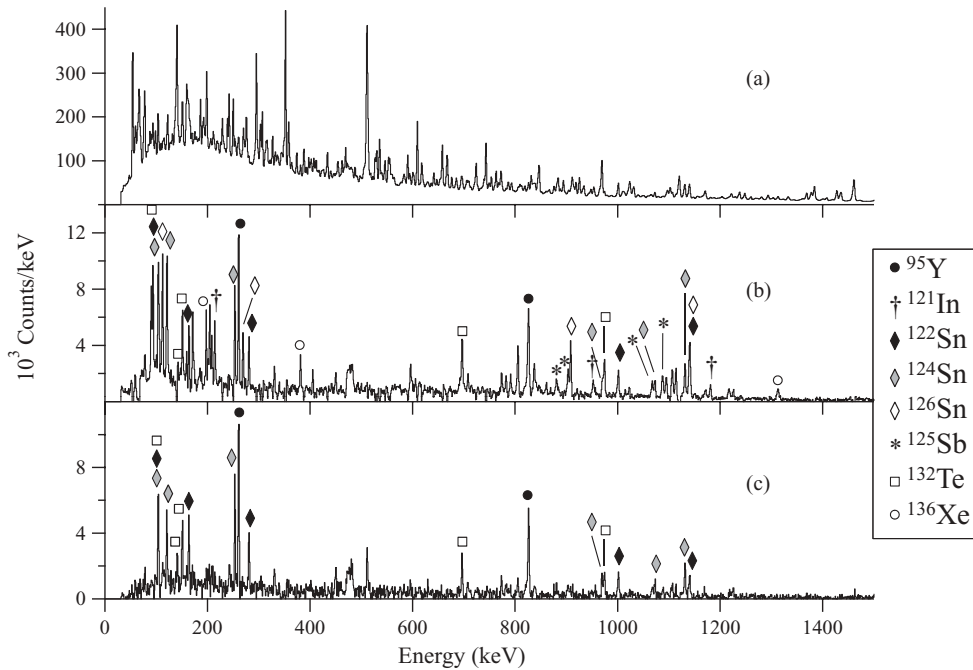


FIG. 1. Delayed  $\gamma$  rays observed in this study. The top panel (a) shows all  $\gamma$  rays in the full 180- $\mu$ s correlation time. This spectrum is dominated by background and  $\beta$ -delayed transitions. The middle panel (b) shows  $\gamma$  rays detected between 5 and 45  $\mu$ s following a particle, with  $\gamma$  rays detected from 130 to 175  $\mu$ s subtracted as a background. Only microsecond isomer transitions are observed. Short-lived isomers ( $\sim$ 5–50  $\mu$ s) dominate. The bottom panel (c) shows  $\gamma$  rays detected between 50 and 100  $\mu$ s following a particle, with  $\gamma$  rays detected from 130 to 175  $\mu$ s subtracted as a background. Isomers with half-lives  $\sim$ 50  $\mu$ s dominate. Peaks associated with select isotopes have been identified. Note that the peak intensity may not be attributed to a single isotope.

with one another, as were 1067 and 902 keV. The 1089- and 1067-keV  $\gamma$  rays are known from  $\beta$ -decay experiments [44] and are assigned as decays from the yrast  $J^\pi = 9/2^+$  and  $11/2^+$  levels to the  $7/2^+$  ground state. Coincidences with the 1067-keV transition are shown in Fig. 4.

The new 880- and 902-keV transitions suggest an isomeric level at 1969 keV, or at a higher excitation energy where the decay was not observed. From a comparison to neighboring Sb isotopes, the latter scheme is proposed. Isomers with  $J^\pi = 19/2^-$  are well known in the odd-Sb nuclei. States with  $15/2^-$  spin often reside at a small energy difference below the  $19/2^-$  level. The proposed decay scheme is shown in Fig. 3.

Delayed transitions, relative to the 902-keV  $\gamma$  ray, were searched for by examining  $\gamma$ - $\gamma$  coincidence times relative to one another. This  $\gamma$ - $\gamma$  relative time window is significantly less than the external clock, at  $\sim$ 135 ns. No delayed transitions within this window were observed coincident with the 902-keV transition.

From the 880- and 902-keV intensities, approximately 60% of the decay flows through the 902–1067-keV decay chain, with the remaining 40% de-exciting through the 880–1089-keV transitions. By using the 902- and 1067-keV transitions, a decay half-life of  $25 \pm 4 \mu$ s is determined for the isomeric decay.

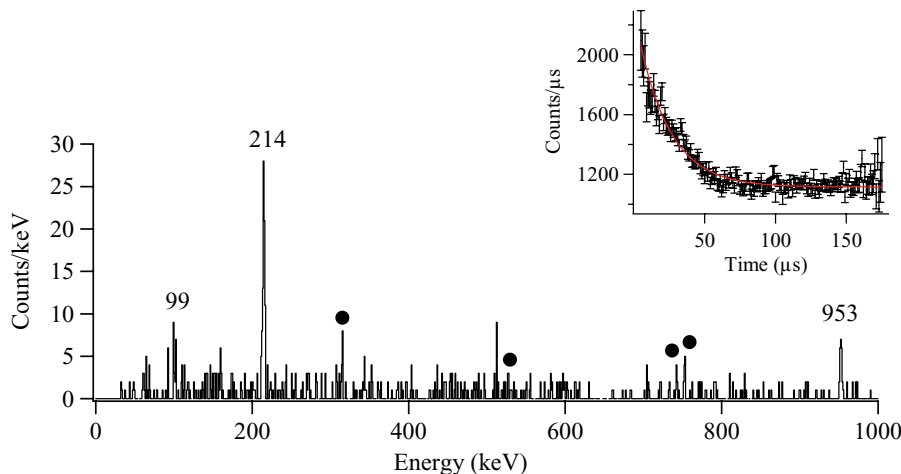


FIG. 2. (Color online)  $\gamma$  rays coincident with 1182 keV, detected within 5–45  $\mu$ s following a particle detected in the Si telescope. An isomeric decay in  $^{121}\text{In}$  dominates the spectrum. The filled circles denote the contaminant peaks from the  $\beta$  decay of  $^{128}\text{Sb}$  ( $T_{1/2} = 9$  h) into  $^{128}\text{Te}$ . The inset shows the  $T_{1/2} = 17(2) \mu$ s decay of the 1182-keV transition.

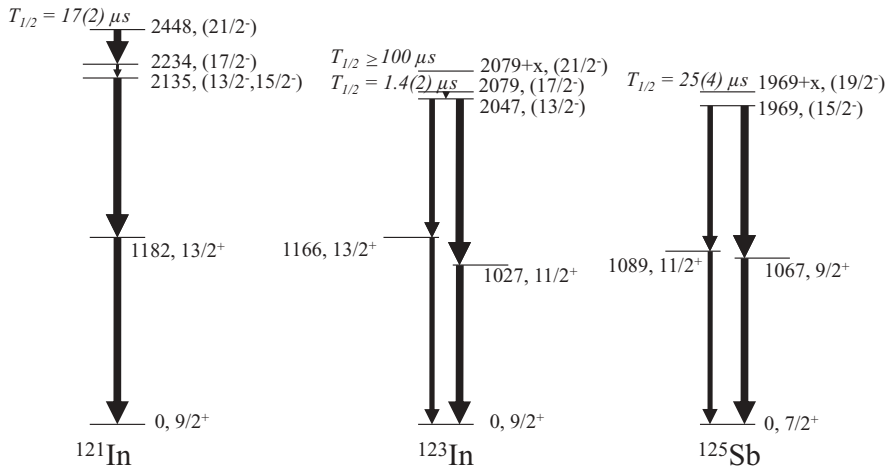


FIG. 3. Proposed decay schemes for the new isomers observed in  ${}^{121,123}\text{In}$  and  ${}^{125}\text{Sb}$ . The 1.4- $\mu\text{s}$  isomer in  ${}^{123}\text{In}$  was measured in Ref. [17]. Additional low-energy decays, not observed in this experiment, are suggested for the isomeric states in  ${}^{123}\text{In}$  and  ${}^{125}\text{Sb}$ .

Decays through the 11/2<sup>-</sup> state at 1890 keV were not observed.

#### IV. DISCUSSION

A number of fission isomers were observed in the  $A \sim 95$ , 122, and 132 mass regions. Characteristics of the isomer decays for each mass distribution are described in more detail in the following discussion.

##### A. Isomers in the $A \sim 95$ Y region

The  $A \sim 95$  mass region has been extensively studied in fission reactions. A number of isomers, notably in the Y isotopes, were observed in this study. Isomer decays assigned to this mass region are typically low in energy and/or a single decay between two long-lived states. Without mass or isotopic separations, assigning observed transitions to particular nuclides is problematic.

A microsecond isomer in  ${}^{92}\text{Y}$  was recently measured in fission products of  ${}^{238}\text{U}$  [45]; however, this decay was not observed in the present experiment. This is likely due to the reported short half-life (4  $\mu\text{s}$ ). Decays with half-lives  $\lesssim 5 \mu\text{s}$  are difficult to observe unless the isomer population is significantly large.

Decays from the 56- $\mu\text{s}$   ${}^{95}\text{Y}$  isomer dominated the isomer spectrum, while the 9- $\mu\text{s}$   ${}^{99}\text{Y}$  isomer was significantly weaker.

A single 257-keV decay from  ${}^{93}\text{Rb}$  is reported in Ref. [7], where isomer population and half-lives were measured in primary fission products following  ${}^{235}\text{U}$  thermal induced fission. Isotope identification was presumably made by x-ray measurements. In subsequent  $\beta$ -decay experiments insensitive to the isomeric half-life [46], the decay energy was adjusted to 253 keV. A more recent  $\beta$ -decay study suggested a half-life of only  $<0.5$  ns for this level [47]. A 253-keV transition was observed in the current work, but it is assigned to the decay from an 8<sup>+</sup> state, fed by a 45(5)- $\mu\text{s}$  isomer, in  ${}^{124}\text{Sn}$ . By assuming two decay components for the 253-keV transition, one with 45  $\mu\text{s}$ , a measured half-life of 60(20)  $\mu\text{s}$  for the second component is determined. This is in excellent agreement with the original work of Ref. [7]. However, the half-life measurement for a single component results in 54(7)  $\mu\text{s}$ , which may be entirely  ${}^{124}\text{Sn}$ . Therefore, the 253-keV decay cannot be unambiguously assigned to  ${}^{93}\text{Rb}$  in this study.

Due to the short  $\beta$ -decay half-lives, transitions assigned to this mass region comprised the bulk of the background events.

##### B. Isomers in the $A \sim 122$ Sn region

A number of isomers attributed to decays in the stable and near-stable Sn isotopes were observed. Nuclear structure studies of the Sn nuclei toward  $N = 82$  are difficult, as the neutron-rich isotopes cannot be populated using standard fusion-evaporation reactions. Isomeric decays were previously

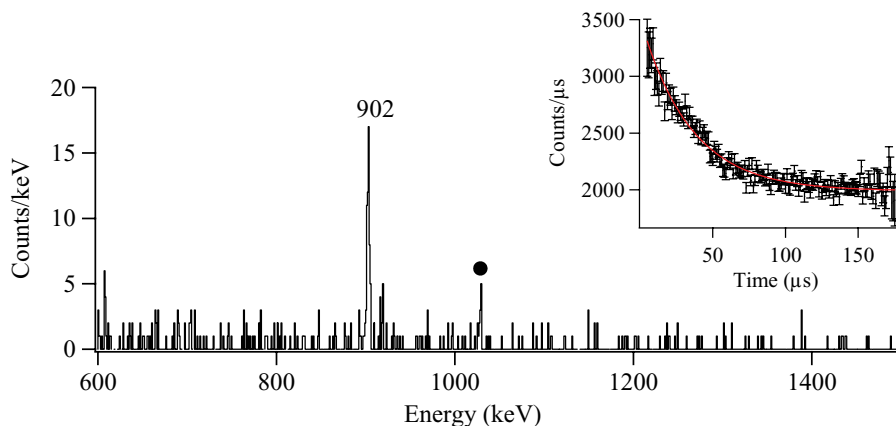


FIG. 4. (Color online)  $\gamma$  rays coincident with 1067 keV, detected within 5–45  $\mu\text{s}$  following a particle detected in the Si telescope. The 902-keV transition is suggested as a decay from isomeric  ${}^{125}\text{Sb}$ . The filled circle denotes the contaminant peak from the  $\beta$  decay of  ${}^{117}\text{Cd}$  ( $T_{1/2} = 3.4$  h) into  ${}^{117}\text{In}$ . The inset shows the  $T_{1/2} = 25(4)$ - $\mu\text{s}$  decay of the 902-keV transition.

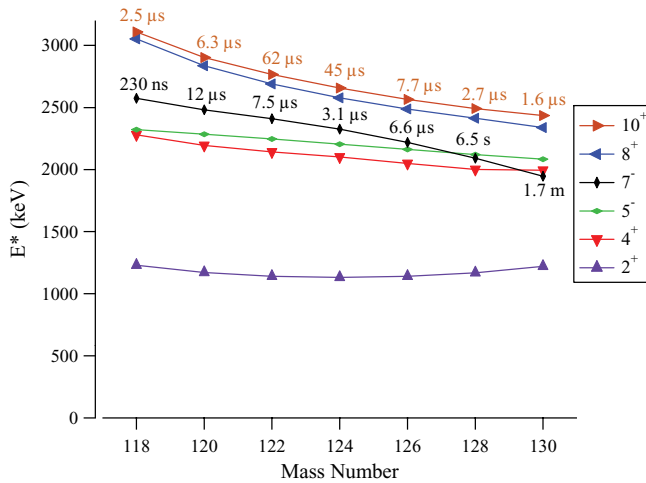


FIG. 5. (Color online) Systematics of energy levels and isomer half-lives in the even Sn isotopes. Decay half-lives for the  $10^+$  and  $7^-$  isomeric states are shown.

measured using light-ion reactions on Cd [20], deep inelastic reactions on stable Sn targets [24,25], and population by In  $\beta$  decay [48]. The current study suggests that intermediate-energy induced fission is another tool for investigating this mass region.

Isomers with  $J^\pi = 10^+$  are observed at  $\sim 3$  MeV in the even-mass  $^{118-130}\text{Sn}$  isotopes. These isomers are attributed to a  $(\nu h_{11/2})^2$  configuration, behaving smoothly with mass number. The decay energies are nearly constant across the mass range, and the half-life reaches a maximum at  $A = 122$  due to the half-filled  $h_{11/2}$  neutron orbital [24,49]. Systematics for level energies and isomer half-lives for the even- $A$  Sn isotopes are shown in Fig. 5.

Negative-parity  $5^-$  and  $7^-$  levels are also observed at low excitation energy in these Sn isotopes. These states involve a coupling between  $1h_{11/2}$  neutrons with the even-parity  $3s_{1/2}$  or  $2d_{3/2}$  orbitals from the  $N = 4$  oscillator shell [50], respectively. As the  $d_{3/2}$  character increases, the  $\nu(h_{11/2} \otimes d_{3/2})7^-$  state is reduced in excitation energy and the isomer half-life increases significantly due to the altered decay path. The  $5^-$  states are also isomeric, but they exhibit much shorter half-lives. Half-lives for the  $5^-$  states decay on the nanosecond time scale, with the longest being 270 ns for  $^{124}\text{Sn}$  [22].

Analogous isomers exist in the odd Sn isotopes, where low-energy states are described as an odd neutron coupled to excitations in the even-even Sn core. Isomers have been assigned to three-quasiparticle configurations of  $(\nu h_{11/2}^2 \otimes \nu s_{1/2})19/2^+$ ,  $(\nu h_{11/2}^2 \otimes \nu d_{3/2})23/2^+$ , and  $(\nu h_{11/2}^3)27/2^-$  [26,27]. With the exception of  $^{123}\text{Sn}$ , the  $27/2^-$  isomers are short-lived ( $< 1 \mu\text{s}$ ) and were not observed in this experiment. In  $^{123}\text{Sn}$ , the reported isomer half-life is  $34 \mu\text{s}$  [21], well within the observation window of the current study. However, decays from this isomer were not observed. Decays from the  $19/2^+$  ( $T_{1/2} = 8 \mu\text{s}$  [18,21]) and  $23/2^+$  ( $T_{1/2} = 6 \mu\text{s}$  [21]) isomers in this isotope were clearly seen.

The  $23/2^+$  isomers are also submicrosecond, except for  $^{129}\text{Sn}$ , where this level has a 2.4- $\mu\text{s}$  half-life [27]. In the odd- $A$  Sn isotopes where this state is known ( $A = 125, 127, 129$ ),

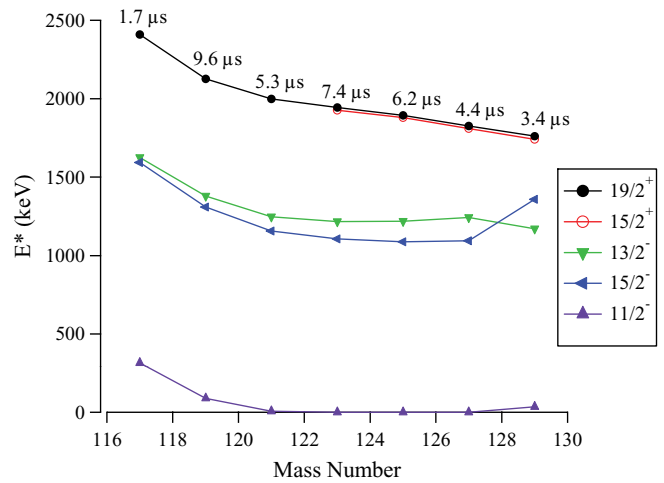


FIG. 6. (Color online) Systematics of energy levels and isomer half-lives in the odd Sn isotopes. Decay half-lives for the  $19/2^+$  isomers are shown.

the  $23/2^+$  levels lie just above the  $19/2^+$  isomer excitation energy.

Figure 6 shows the populated levels below the  $19/2^+$  isomeric states. As mentioned previously, these states are suggested to arise predominantly from  $\nu h_{11/2}^2 \otimes \nu s_{1/2}$ , corresponding to the odd neutron coupled to the  $5^-$  excitation in the even-even Sn core. In the even-even Sn isotopes, the  $5^-$  levels predominantly  $E1$  decay to the  $(\nu h_{11/2}^2)4^+$  states. In the neighboring odd isotopes, the  $(4^+ \otimes \nu h_{11/2})17/2^-$ ,  $19/2^-$  states lie higher in excitation energy, above the  $19/2^+$  level. The  $19/2^+$  states therefore decay through the  $(2^+ \otimes \nu h_{11/2})13/2^-$ ,  $15/2^-$  states via  $E3$  and  $M2$  transitions, respectively. These decays are significantly hindered, as mixing with far-lying, shell-model orbitals is necessary. For example, the  $M2$  decay requires admixtures of the  $\nu 1g_{7/2}$  orbital, while the  $E3$  necessitates admixtures of the  $\nu 2d_{5/2}$  character. In  $^{123-129}\text{Sn}$ , additional levels with  $J^\pi = 15/2^+$  are also suggested to lie near the  $19/2^+$  isomers. The very low energy difference between these states also inhibits prompt decays.

Isomers attributed to similar shell-model states have also been identified in  $Z = 51$  Sb isotopes. Low-energy excited states in the odd mass Sb isotopes arise from the odd proton occupying the  $2d_{5/2}$  ( $5/2^+$ ),  $2g_{7/2}$  ( $7/2^+$ ), and  $1h_{11/2}$  ( $11/2^-$ ) orbitals. Isomers with spins  $J^\pi = 15/2^-$  and  $19/2^-$  have been attributed to the odd-proton coupling to the  $5^-$  and  $7^-$  states in the even-even Sn core [31]. Note that these are not pure shell-model states and have significant admixtures of other configurations.

In the odd-odd Sb isotopes, the decay energies are typically very low ( $< 100$  keV) and cannot be observed in the current experiment.

The odd-proton  $Z = 49$  isotopes also have numerous isomers, where the  $\pi g_{9/2}$  hole couples to neutron excitations similar to what has been observed in the Sn and Sb isotopes. Recent work has highlighted high-spin isomers in the odd mass  $A = 119-129$  nuclei [17,43,51]. By analogy with the Sb isotopes, isomers with  $J^\pi = 17/2^-$  and  $21/2^-$ , from the

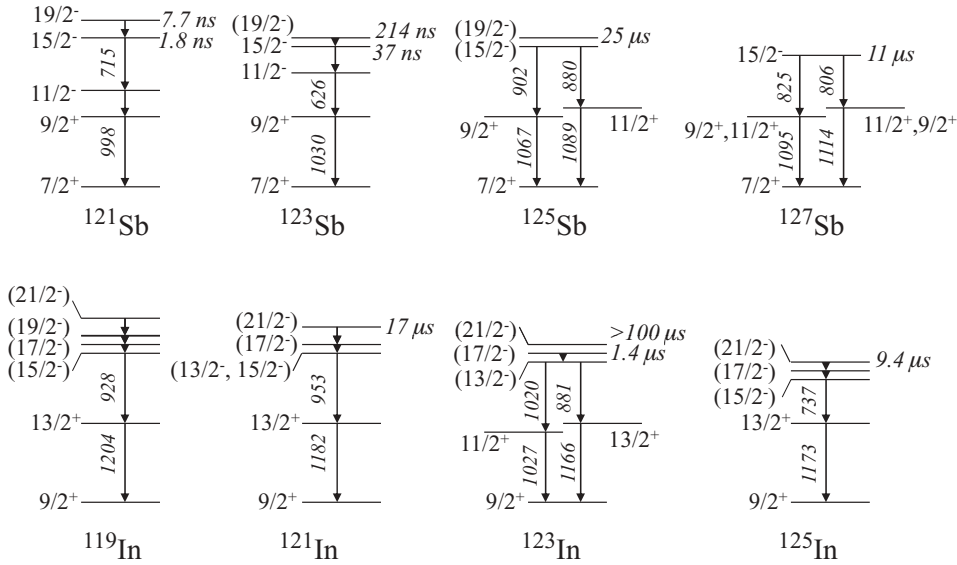


FIG. 7. Systematics of energy levels and isomer half-lives in the odd Sb and In isotopes with  $N = 70$ – $76$ . Decay energies greater than 500 keV are shown. Data are from Refs. [17,30,32,43] and this work.

odd-proton coupling to the  $5^-$  and  $7^-$  neutron excited states, are expected.

The isomeric structure in this mass region is dominated by the  $5^-$  and  $7^-$  two-quasiparticle neutron excitations. As mentioned earlier, these neutron configurations are the foundation for long-lived states in  $N = 76$ – $78$  nuclei with a closed proton shell ( $Z = 50$  Sn), as well as neighboring nuclei with a valence neutron (odd- $A$  Sn), or valence proton (odd- $A$  Sb and In). In the even- $A$  Sn isotopes, the  $7^-$  level gradually lowers in excitation energy relative to the  $5^-$  state. At  $N = 78$ , the  $7^-$  falls below the  $5^-$  level. This inversion is also observed in the odd-proton nuclei. In the Sb (In) isotopes, the lowering of the  $19/2^-$  ( $21/2^-$ ) relative to the  $15/2^-$  ( $17/2^-$ ) states occurs, reversing the order in excitation energy at  $N = 78$ . The  $19/2^-$  level in  ${}^{129}\text{Sb}$   $\beta$  decays with a 18-min half-life; similarly for  ${}^{127}\text{In}$ , the  $21/2^-$  level is a  $\beta$ -decaying isomer with a 1-s half-life.

The Sb and In isotopes make an interesting comparison, with one-proton particle and hole outside of the closed  $Z = 50$  closed shell. While the  $5^-$  and  $7^-$  neutron excitations dominate the isomeric landscape, the half-lives and decay systematics are not as smooth as the  $Z = 50$  Sn due to additional levels that allow alternate decay paths. Systematics of the  $N = 70$ – $76$  In and Sb isotopes are shown in Fig. 7. Similar to the odd- $A$  Sn, the high-spin states attributed to the  $5^-$  and  $7^-$  neutron configurations decay through levels associated with  $2^+$  neutron excitations as the  $4^+$  excitations lie higher in energy and are unavailable.

In the Sb isotopes with  $N \leq 74$ , the single-particle  $\pi h_{11/2}$  level lies below the  $J^\pi = 15/2^-$  and  $19/2^-$  states. The  $15/2^-$  states can readily  $E2$  decay to this level as compared to the hindered  $M2$  and  $E3$  decays to the  $11/2^+$  and  $9/2^+$  states, respectively. In the heavier Sb isotopes, the  $\pi h_{11/2}$  increases in excitation energy, and the  $15/2^-$  decay can no longer decay through this level. In  ${}^{127}\text{Sb}$ , the  $J^\pi = 15/2^-$  state is a microsecond isomer [32] and the excitation energy of the  $19/2^-$  level is unknown.

Additional high-spin states are also observed in the In isotopes. However, a high-spin, proton single-particle state,

similar to the  $\pi h_{11/2}$  orbital in the Sb isotopes, is not available at low energy. A cluster of negative-parity states exist at  $\sim 2$  MeV, and low-energy decays (often  $< 100$  keV) are observed between these states. In the  $N = 70$ – $76$  isotopes, a  $J^\pi = 13/2^-$  or  $15/2^-$  lies below the  $21/2^-$  and  $17/2^-$ ; the low-energy difference preserves the isomeric nature of these levels.

The isomeric structure observed in the In, Sn, and Sb isotopes rapidly disappears. Similar isomers are not consistently observed further from the  $Z = 50$  closed shell. The spherical structure is quickly replaced by collective vibrations in Te ( $Z = 52$ ) and Cd ( $Z = 48$ ).

### C. Isomers in the $A \sim 132$ Xe region

As the complement to the light  $A \sim 95$  fragments, the  $A \sim 132$  region is also well populated in the fission reaction.

The  ${}^{134}\text{Xe}$  and  ${}^{136}\text{Xe}$  isomers are easily observed despite the short half-lives, as the isomer population in the fission reaction is significant. With a closed neutron shell,  $N = 82$   ${}^{136}\text{Xe}$  displays a spherical structure with a pair of  $1g_{7/2}$  protons coupling to form the  $J_{\text{max}} = 6^+$  isomeric state at 1892 keV. The lighter xenon isotopes quickly assume vibrational character, although  ${}^{132,134}\text{Xe}$  still have significant single-particle contributions [52].

Both  ${}^{132}\text{Xe}$  and  ${}^{134}\text{Xe}$  have  $7^-$  and  $10^+$  isomers, attributed to neutron excitations of  $\nu h_{11/2} \otimes \nu d_{3/2}$  and  $(\nu h_{11/2})^2$ , respectively, similar to what is observed in the even- $A$  Sn isotopes. In  ${}^{132}\text{Xe}$ , these isomers are out of range to be observed in the current experiment—the  $7^-$  half-life is too short (87 ns [53–55]), while the  $10^+$  is too long (8.4 ms [56]). In  ${}^{134}\text{Xe}$ , the opposite is nearly true; the  $7^-$  half-life is long (290 ms [57]) while the  $10^+$  is short (5  $\mu\text{s}$  [37]). However, the large population of  ${}^{134}\text{Xe}$  in fission permits observation of the  $10^+$  isomeric decay.

Isomers in the  $Z = 52$  Te isotopes also exist for the  $N = 78$  and  $N = 80$  isotones. In  ${}^{128}\text{Te}$ , decays from the  $T_{1/2} = 28$ - $\mu\text{s}$   $7^-$  isomer [36] are readily observed. However,

transitions following the  $3.7\text{-}\mu\text{s}$   $10^+$  isomer [37,58] were too weak to be seen in this study. The  $7^-$  and  $10^+$  isomers in  $^{130}\text{Te}$  are relatively short-lived, at 115 ns and  $1.9\ \mu\text{s}$ , respectively [37,59]. Both of these decays are outside of the detection window.

A  $J^\pi = 19/2^-, 24\text{-}\mu\text{s}$  isomer has been recently identified in  $Z = 53$   $^{131}\text{I}$  [34], and this decay is confirmed in the current paper. A half-life of  $24(4)\ \mu\text{s}$  was determined from the 330-, 778-, and 782-keV transitions in the current paper, in excellent agreement with Ref. [34]. The isomeric state is suggested to arise from the coupling of the odd  $g_{7/2}$  proton to  $J^\pi = 7^-$  neutron excitations; this neutron configuration commonly produces isomeric states, as discussed earlier, in the neighboring even- $Z$  nuclei.

## V. CONCLUSIONS

In summary, isomers in primary fragments from the induced fission of  $^6\text{Li}$  on  $^{232}\text{Th}$  were populated and examined. Isomeric decays from both the symmetric and antisymmetric fission distribution were observed. Antisymmetric fission produced well-known isomers in the  $A \sim 95$  and  $A \sim 132$  mass regions, while symmetric fission probed the  $A \sim 122$  nuclei near  $Z = 50$ .

Nuclear structure studies of this latter region are challenging, as production reactions are limited. The use of energetic fission to populate and observe isomeric decays has been demonstrated to be a successful method for probing these hard-to-reach isotopes.

Isomeric decays with a range of half-lives can be investigated with the current technique. Short-lived isomers can be observed between the cyclotron pulses ( $\sim 125$  ns), while the electrostatic deflector may be used for longer lived decays. Future work will take advantage of the flexible timing setup to explore submicrosecond decay half-lives for isomeric states in the fission fragments.

The current paper investigated microsecond isomers with half-lives  $\sim 5\text{--}100\ \mu\text{s}$ . New isomers in  $^{121}\text{In}$ ,  $^{123}\text{In}$ , and  $^{125}\text{Sb}$  are presented. These isomers are suggested to arise from the odd-proton coupling to  $5^-$  and  $7^-$  neutron core excitations. In both  $^{123}\text{In}$  and  $^{125}\text{Sb}$ , low-energy transitions not observed in the

current paper are proposed in the decay of the isomeric state. Further studies to elucidate the structure of these nuclides, as well as  $^{121}\text{In}$ , are needed. Of particular need are measurements of the low-energy transitions; this may be accomplished by utilizing a  $\gamma$ -detector array with high efficiency at low energy and/or electron spectroscopy. A higher efficiency HPGe array (such as Gammasphere) would also be useful, particularly with the addition of low-energy sensitive detectors.

Fission fragment isomer spectroscopy would also benefit from the inclusion of mass separation. This would clarify identification of the fragments emitting only a single  $\gamma$  decay from the isomeric state. In addition, isomers that do not decay to previously known states may also be characterized. In many instances,  $\gamma$  detectors may be placed at the target station as well as the focal plane of a fragment separator. This would allow states both above and below isomeric states to be coupled using isomer decay tagging, and more complete spectroscopic studies to be undertaken (see, for example, Refs. [60–64]).

Broader isomeric searches may be accomplished with alternative targets. In antisymmetric fission, the heavy fragment mass distribution remains relatively constant for a range of fissioning systems. The lighter fragment, however, can be significantly affected. Use of a heavier actinide target will produce a higher mass fragment distribution, while lighter targets will populate lower masses. Induced fission experiments on lighter targets, for example Pb or Bi, may probe new isomers in the neutron-rich region near  $A \sim 90$ .

## ACKNOWLEDGMENTS

The authors thank the 88-Inch Cyclotron operations and facilities staff for the experimental support of this study. We would also like to thank J. Greene of Argonne National Laboratory for the preparation of the  $^{232}\text{Th}$  target. We are grateful to the Department of Energy's NNSA, Office of Nonproliferation Research and Development (NA-22), for financial support. This work was performed under the auspices of the US Department of Energy under Contract Nos. DE-AC05-76RLO-1830 (PNNL), DE-AC52-07NA27344 (LLNL), and DE-AC02-05CH11231 (LBNL).

- 
- [1] H. Freiesleben, G. T. Rizzo, and J. R. Huizenga, *Phys. Rev. C* **12**, 42 (1975).
  - [2] S. R. Lesher *et al.* (submitted to *Nucl. Instrum. Methods A*).
  - [3] J. T. Harke *et al.*, *Phys. Rev. C* **73**, 054604 (2006).
  - [4] G. Duchêne, F. A. Beck, P. J. Twin, G. de France, D. Curien, L. Hana, C. W. Beausang, M. A. Bentley, P. J. Nolan, and J. Simpson, *Nucl. Instrum. Methods Phys. Res. A* **432**, 90 (1999).
  - [5] Z. Elekes, T. Belgya, G. L. Molnár, A. Z. Kiss, M. Csatlós, J. Gulvás, A. Krasznahorkay, and Z. Máté, *Nucl. Instrum. Methods Phys. Res. A* **503**, 580 (2003).
  - [6] I. M. Itkis *et al.*, *Phys. Lett.* **B640**, 23 (2006).
  - [7] J. W. Grüter, K. Sistemich, P. Armbruster, J. Eidens, and H. Lawin, *Phys. Lett.* **B33**, 474 (1970).
  - [8] J. Genevey, F. Ibrahim, J. A. Pinston, H. Faust, T. Friedrichs, M. Gross, and S. Oberstedt, *Phys. Rev. C* **59**, 82 (1999).
  - [9] J. W. Grüter, *JUL-879-NP* (1972).
  - [10] B. Proot and J. Uyttenhove, *Nucl. Instrum. Methods* **192**, 447 (1982).
  - [11] E. Monnard *et al.*, in 3rd International Conference on Nuclei Far from Stability, Cargese, Corsica, Abstr. A26 (1976).
  - [12] R. B. Walton and R. E. Sund, *Phys. Rev.* **178**, 1894 (1969).
  - [13] R. A. Meyer, E. Monnard, J. A. Pinston, F. Schussler, I. Ragnarsson, B. Pfeiffer, H. Lawin, G. Lhersonneau, T. Seo, and K. Sistemich, *Nucl. Phys.* **A439**, 510 (1985).
  - [14] H. Bartsch, K. Huber, U. Kneissl, and H. Krieger, *Z. Phys.* **A 285**, 273 (1978).
  - [15] M. Bini, A. M. Bizzeti-Sona, P. Blasi, M. Lorini, and N. Taccetti, *Phys. Rev. C* **21**, 116 (1980).
  - [16] D. J. Martin and S. A. Wender, *J. Phys. G* **4**, 1347 (1978).
  - [17] A. Scherillo, J. Genevey, J. A. Pinston, A. Covello, H. Faust, A. Gargano, R. Orlandi, G. S. Simpson, I. Tsekhanovich, and N. Warr, *Phys. Rev. C* **70**, 054318 (2004).



- [18] R. H. Mayer *et al.*, *Z. Phys. A* **342**, 247 (1992).
- [19] H. Ikegami, *Phys. Rev.* **120**, 2185 (1960).
- [20] S. Lunardi, P. J. Daly, F. Soramel, C. Signorini, B. Fornal, G. Fortuna, A. M. Stefanini, R. Broda, W. Meczynski, and J. Blomqvist, *Z. Phys. A* **328**, 487 (1987).
- [21] P. J. Daly *et al.*, *Phys. Scr.* **T56**, 94 (1995).
- [22] B. Fogelberg and P. Carlé, *Nucl. Phys.* **A323**, 205 (1979).
- [23] H. C. Cheung, H. Huang, and J. K. P. Lee, *Can. J. Phys.* **57**, 460 (1979).
- [24] R. Broda *et al.*, *Phys. Rev. Lett.* **68**, 1671 (1992).
- [25] R. H. Mayer *et al.*, *Phys. Lett.* **B336**, 308 (1994).
- [26] J. A. Pinston, C. Foin, J. Genevey, R. Béraud, E. Chabanat, H. Faust, S. Oberstedt, and B. Weiss, *Phys. Rev. C* **61**, 024312 (2000).
- [27] R. L. Lozeva *et al.*, *Phys. Rev. C* **77**, 064313 (2008).
- [28] C. T. Zhang, P. Bhattacharyya, P. J. Daly, Z. W. Grabowski, R. Broda, B. Fornal, and J. Blomqvist, *Phys. Rev. C* **62**, 057305 (2000).
- [29] H. Gausemel, B. Fogelberg, T. Engeland, M. Hjorth-Jensen, P. Hoff, H. Mach, K. A. Mezilev, and J. P. Omtvedt, *Phys. Rev. C* **69**, 054307 (2004).
- [30] H. Watanabe *et al.*, *Phys. Rev. C* **79**, 024306 (2009).
- [31] G. A. Jones *et al.*, *Phys. Rev. C* **77**, 034311 (2008).
- [32] K. E. Apt and W. B. Walters, *Phys. Rev. C* **9**, 310 (1974).
- [33] J. W. Borgs, H.-P. Kohl, G. Lhersonneau, H. Ohm, U. Paffrath, K. Sistemich, D. Weiler, and R. A. Meyer, *Nucl. Instrum. Methods B* **26**, 304 (1987).
- [34] H. Watanabe *et al.*, *Phys. Rev. C* **79**, 064311 (2009).
- [35] J. McDonald and A. Kerek, *Nucl. Phys.* **A206**, 417 (1973).
- [36] K. Sistemich, W.-D. Lauppe, H. Lawin, F. Schussler, J. P. Bocquet, F. Monnard, and J. Blomqvist, *Z. Phys. A* **292**, 145 (1979).
- [37] J. Genevey, J. A. Pinston, C. Foin, M. Rejmund, R. F. Casten, H. Faust, and S. Oberstedt, *Phys. Rev. C* **63**, 054315 (2001).
- [38] L. C. Carraz, J. Blachot, E. Monnard, and A. Moussa, *Nucl. Phys.* **A158**, 403 (1970).
- [39] W. John, F. W. Guy, and J. J. Wesolowski, *Phys. Rev. C* **2**, 1451 (1970).
- [40] R. G. Clark, L. E. Glendenin, and W. L. Talbert Jr., in *Proceedings of the Third IAEA Symposium on the Physics and Chemistry of Fission, Rochester, NY, 1973* (IAEA, Vienna, 1974), Vol. 2, p. 221.
- [41] B. Fogelberg and P. Hoff, *Nucl. Phys.* **A376**, 389 (1982).
- [42] J. W. Smits and R. H. Siemssen, *Nucl. Phys.* **A261**, 385 (1976).
- [43] R. Lucas *et al.*, *Eur. Phys. J. A* **15**, 315 (2002).
- [44] J. Katakura, *Nucl. Data Sheets* **86**, 955 (1999).
- [45] C. M. Folden III *et al.*, *Phys. Rev. C* **79**, 064318 (2009).
- [46] C. Baglin, *Nucl. Data Sheets* **80**, 1 (1997).
- [47] K. Sistemich, K. Kawade, H. Lawin, G. Lhersonneau, H. Ohm, U. Paffrath, V. Lopac, S. Brant, and V. Paar, *Z. Phys. A* **325**, 139 (1986).
- [48] B. Fogelberg, K. Heyde, and J. Sau, *Nucl. Phys.* **A352**, 157 (1981).
- [49] J. J. Ressler *et al.*, *Phys. Rev. C* **69**, 034317 (2004).
- [50] K. Krien, B. Klemme, R. Folle, and E. Bodenstedt, *Nucl. Phys.* **A228**, 15 (1974).
- [51] J. Genevey, J. A. Pinston, H. R. Faust, R. Orlandi, A. Scherillo, G. S. Simpson, I. S. Tsekhanovich, A. Covello, A. Gargano, and W. Urban, *Phys. Rev. C* **67**, 054312 (2003).
- [52] C. Goodin, J. R. Stone, N. J. Stone, A. V. Ramayya, A. V. Daniel, J. H. Hamilton, K. Li, J. K. Hwang, G. M. Ter-Akopian, and J. O. Rasmussen, *Phys. Rev. C* **79**, 034316 (2009).
- [53] J. J. Valiente-Dobón *et al.*, *Phys. Rev. C* **69**, 024316 (2004).
- [54] D. A. Volkov, B. I. Gorbachev, A. I. Kovalenko, A. I. Levon, O. F. Nemets, and O. V. Sevastyuk, *Yad. Fiz.* **44**, 849 (1986).
- [55] A. Kerek, A. Luukko, M. Grecescu, and J. Sztarkier, *Nucl. Phys.* **A172**, 603 (1971).
- [56] M. v. Hartrott, J. Hadijuana, K. Nishiyama, D. Quitmann, D. Riegel, and H. Schweickert, *Z. Phys. A* **278**, 303 (1976).
- [57] W. G. Winn, Ph.D. thesis, Cornell University, 1968.
- [58] C. T. Zhang *et al.*, *Nucl. Phys.* **A628**, 386 (1998).
- [59] K. Kerek, P. Carlé, and J. McDonald, *Nucl. Phys.* **A198**, 466 (1972).
- [60] D. M. Cullen *et al.*, *Phys. Rev. C* **58**, 846 (1998).
- [61] J. J. Ressler *et al.*, *Phys. Rev. C* **63**, 067303 (2001).
- [62] D. M. Cullen *et al.*, *Phys. Lett.* **B529**, 42 (2002).
- [63] W. Królas *et al.*, *Phys. Rev. C* **65**, 031303(R) (2002).
- [64] J. J. Ressler *et al.*, *Phys. Rev. C* **69**, 034331 (2004).